Journal of Power Sources 556 (2023) 232412

Contents lists available at ScienceDirect

Journal of Power Sources

journal homepage: www.elsevier.com/locate/jpowsour

An electrochemical evaluation of state-of-the-art non-flammable liquid electrolytes for high-voltage lithium-ion batteries

Florian Gebert [a], Matilde Longhini [a,b], Fosca Conti [b], Andrew J. Naylor [a,*]

[a] Department of Chemistry – Ångström Laboratory, Uppsala University, SE-75121, Uppsala, Sweden
[b] Department of Chemical Sciences, University of Padova, Via Marzolo 1, 35131, Padova, Italy

HIGHLIGHTS

- Hydrofluorocarbon electrolytes perform better than phosphates/phosphonates.
- Greater capacity retention and rate capability is displayed for hydrofluorocarbons.
- Resistance measurements point to inferior interphases with phosphates/phosphonates.

GRAPHICAL ABSTRACT

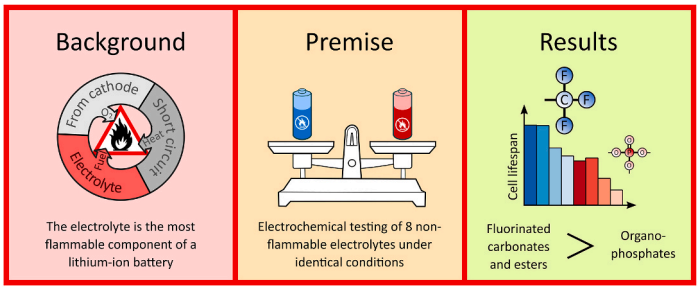

ARTICLE INFO

Keywords:
Lithium-ion battery
Non-flammable electrolyte
NMC

ABSTRACT

The rapid and accelerating adoption of lithium-ion batteries worldwide, especially in the transportation sector, has focused attention on their safety. One area of particular interest is finding alternatives for their most flammable component, the liquid electrolyte. Over the past 20 years, a number of non-flammable liquid electrolytes have been identified and tested. However, because these data are frequently obtained under a wide range of conditions – e.g., different active materials, current densities or voltage cutoffs – it is difficult to compare them. In this work, eight promising non-flammable liquid electrolytes – four phosphate derivatives and four based on fluorinated hydrocarbons – are identified from the literature and tested in commercially relevant high-voltage systems under identical conditions. The electrochemical stabilities of the electrolytes were studied against both inert electrodes and in $LiNi_{0.6}Mn_{0.2}Co_{0.2}O_2$|graphite cells. Each electrolyte was assessed via long-term cycling experiments and rate-testing and the cell resistance during aging was monitored. It was found that the electrolytes containing phosphate and phosphonate-based solvents generally performed very poorly compared to the phosphorus-free fluorinated solvents; the latter resulted, on average, in twice the capacity retention after 500 cycles of the former. A strong correlation was observed between long-term cycling performance, rate capability and the cell resistance.

* Corresponding author.
E-mail address: andy.naylor@kemi.uu.se (A.J. Naylor).

https://doi.org/10.1016/j.jpowsour.2022.232412
Received 31 August 2022; Received in revised form 25 October 2022; Accepted 13 November 2022
Available online 25 November 2022

1. Introduction

Over the past decade, a broad consensus has emerged that the fossil-fuel powered cars and trucks that currently account for most of the world's vehicle fleet will have to be replaced in large part by electric vehicles (EVs) running on lithium-ion batteries (LIBs) [1,2]. This transition will have clear positive environmental and public health benefits. EVs are also very safe: although the sample size is still much too small for a rigorous comparison, EV fires have so far occurred at lower rates than in combustion vehicles [3]. Nevertheless, it is crucial to minimize such accidents – both as an imperative in its own right and to maintain public confidence in the technology. The strenuous conditions of use to which EV batteries are subjected – wide temperature ranges, frequent physical shocks and rapid charging and discharging – increase their susceptibility to failures that could cause thermal runaway [4]. It is also worth noting that current LIBs, even when sealed and undamaged, potentially contain all the components required for fire: oxygen, fuel and heat. Oxygen is stored in the lattice of the cathode materials and can be released as O_2 during cathode decomposition. The highly flammable liquid electrolytes represent the most important potential fuel for a fire, but the separator [5], plastic packaging and electrode materials can also undergo exothermic decompositions [6]. Finally, the considerable energy storable in an EV cell can be converted quickly into heat upon a short circuit in the cell.

A great deal of effort has gone into managing or reducing the flammability risk of LIBs. At the cell or pack level, this often involves venting systems, more durable separators [7] or switching to a more thermally stable active material like lithium iron phosphate [8]. At the materials level, research has gone into reducing the flammability of electrolytes, which are by far the most flammable components of LIBs [9]. The most widely-used LIB electrolytes today are composed of solutions of $LiPF_6$ in organic carbonate esters – usually ethylene carbonate (EC) mixed with one or more linear carbonate like diethyl carbonate (DEC) or ethyl methyl carbonate (EMC). These have been in wide use since the commercialization of LIBs in the 1990s and have seen decades of refinement and characterization since then. As a result, they are well-understood and considered highly reliable. However, they are also highly flammable, with heats of combustion of -10 to -15 kJ g^{-1} [10], comparable to coal lignite [11]. As a result, there is significant interest in replacing these electrolytes with less flammable alternatives. One possibility is solid-state electrolytes, which have the advantage of also potentially improving energy density. Although they have recently been the focus of intense interest and may yet see commercialization, they are far from mature as they pose considerable processing or manufacturing challenges and therefore high costs [12]. Ionic liquids, another popular option, are also held back by potentially high costs and poor Li^+ transport properties [13].

Nonaqueous liquid electrolytes represent the most feasible near-term non-flammable electrolytes. They are mainly dominated by two classes of compounds: organophosphorus compounds, which include phosphates, phosphites, phosphazenes and phosphonates (and sometimes fluorinated versions thereof); and hydrofluorocarbons, which include fluorinated carbonates, esters and ethers. The organophosphorus class has the advantage of being cheap, but poses unresolved interfacial problems with graphite electrodes [14], although a variety of strategies, mostly using additives, have been proposed to improve this. It is interesting to note that in sodium-ion batteries, which typically contain hard carbon rather than graphite anodes, organophosphorus compounds do not exhibit these issues and have shown highly promising cycling stability [15,16]. Fluorinated carbonates, esters and ethers are more readily compatible with graphite, as they often form electrically insulating and ionically conductive solid-electrolyte interphases (SEIs). However, they are considerably more expensive and associated with safety concerns related to toxic decomposition products, particularly hydrogen fluoride. There are also environmental concerns around their synthesis [17] and end-of-life treatment [18].

Although some work has been published studying candidates for non-flammable liquid electrolytes, they have been tested under a range of different conditions. Electrode materials, salts and salt concentrations, voltage cutoffs, C-rates and temperatures often vary across studies. In this work, several techniques are used to investigate, under identical conditions, the electrochemical performance of eight promising previously reported candidates for non-flammable LIB electrolytes. The electrolytes were employed in commercially-relevant high-voltage $LiNi_{0.6}Mn_{0.2}Co_{0.2}O_2$ (NMC622)|graphite cells to provide a realistic system for comparison. Only widely-used solvents that have been shown to be significantly less flammable than traditional carbonate esters – as measured by self-extinguishing time, onset of thermal runaway or heat of combustion – were considered. The electrolytes were selected considering real-world viability, focusing on systems with moderate salt concentrations and which have been reported to work well in graphite-containing cells. Highly concentrated electrolytes, a popular recent strategy for reducing flammability and improving cycling performance, were not considered, as they are judged to come with high costs [19], which will likely eventually render them commercially uncompetitive.

This study employs linear sweep voltammetry (LSV) to assess the electrochemical stability window of each electrolyte, as well as galvanostatic cycling and rate-testing to understand long-term performance, and intermittent current interruption (ICI) to determine cell resistance at particular states of charge.

2. Results and discussion

Eight non-flammable solvent systems were examined in this study. Table 1 summarizes their compositions and flammability characteristics. Where available, co-solvents or additives reported to improve a given solvent's performance were used. In the cases of TFEC, TFEP and TTE, such co-solvents are necessary because $LiPF_6$ is not soluble in the non-flammable solvent alone. Mixtures of ethylene carbonate (EC) with a linear carbonate ester (e.g., diethyl carbonate (DEC) or ethylmethyl carbonate (EMC)) are widely-used co-solvents. Propylene carbonate (PC) and γ-butyrolactone (GBL) are also interesting, as they are less volatile and thus less flammable than traditional linear carbonates [20]. As a standard electrolyte, LP57 was chosen, a widely-used commercial electrolyte consisting of 1 M $LiPF_6$ in a 3:7 v/v mixture of EC and EMC. To maintain identical experimental conditions throughout the study, the cycling regime including choice of cut-off voltage and C-rate, as well as electrolyte volume and temperature among other parameters, were kept constant.

LSV was conducted to study the electrochemical stability windows; the hydrofluorocarbon-based (Fig. 1a) and phosphate/phosphonate-based electrolytes (Fig. 1b) are plotted separately to preserve readability. Carbon-coated aluminium and carbon-coated copper working electrodes were used for the cathodic and anodic sweeps, respectively, to simulate the current collectors used for LIB cathodes and anodes. The tested voltage window was selected based on the operating ranges of typical high-voltage LIBs, in which the lower cutoff is usually set at 3 V (corresponding to ca. 2 V for graphite vs Li/Li^+) and the upper cutoff at 4.5–5 V (corresponding to just above 0 V vs Li/Li^+ for graphite). As shown in the insets in Fig. 1a and b, all eight electrolytes exhibit a small peak at ca. 1 V with a magnitude of ca. -15 μA cm^{-2} during the anodic sweep, which is probably related to SEI formation reactions. The current density only becomes significantly more negative at ca. 0.1 V, but still does not surpass -100 μA cm^{-2}, suggesting that the electrolytes are largely anodically stable. During the cathodic sweep, some electrolytes show signs of significant instability, starting with MFA at 4.8 V. Several – notably FEMC:FEC, FEC:TTE, PC:TFEC and EC:DEC:TFEP – show only low currents of less than approximately <10 μA cm^{-2} throughout the voltage range tested (0–6 V). With some exceptions, the oxidation peaks produced by the phosphate/phosphonate-based electrolytes are much more pronounced than those of the hydrofluorocarbons, although this may be related to the much greater proportion of co-solvents present in

Table 1
Descriptions of the non-flammable solvent systems studied in this work. Abbreviations: ARC = accelerated rate calorimetry, DSC = differential scanning calorimetry, SET = self-extinguishing time, FP = flash point. Pass/fail refers to a visual inspection of the burning behavior after being exposed to a flame source. All ratios of liquid mixtures are vol/vol; solid additives refer to mass/mass relative to the total amount of $LiPF_6$ in the electrolyte.

Non-flammable solvent	Co-solvent	Additives	Characterization of flammability
2,2,2-trifluoroethyl methyl carbonate (FEMC)	10 vol% fluoroethylene carbonate (FEC) [21,22]	None	Pass/fail [23], ARC [22,24]
1,1,2,2-tetrafluoroethyl-2,2,3,3-tetrafluoropropylether (TTE)	60 vol% FEC [22]	None	ARC [22]
Methyl difluoroacetate (MFA)	None [25–29]	2 vol% vinylene carbonate (VC) [28,29]	DSC [25,26,28–30]
Bis(2,2,2-trifluoroethyl) carbonate (TFEC)	30 vol% propylene carbonate (PC) [31–33]	1 vol% FEC [33]	SET [33], FP [33]
Tris(2,2,2-trifluoroethyl) phosphate (TFEP)	70 vol% EC:DEC (1:1) [34]	None	SET [34,35], DSC [36,37]
Trimethyl phosphate (TMP)	70 vol% GBL (γ-butyrolactone) [38]	3 wt% lithium difluoro(oxalate) borate (LiODFB) [38]	SET [38]
	80 vol% GBL [39]	2 vol% VC + 5 vol% vinyl ethylene carbonate (VEC) [39]	Pass/fail [40], SET [20,41–43]
Dimethyl methylphosphonate (DMMP)	90 vol% EC:DEC (1:1) [44]	5 wt% lithium bis(oxalato)borate (LiBOB) [44]	SET [44,45]

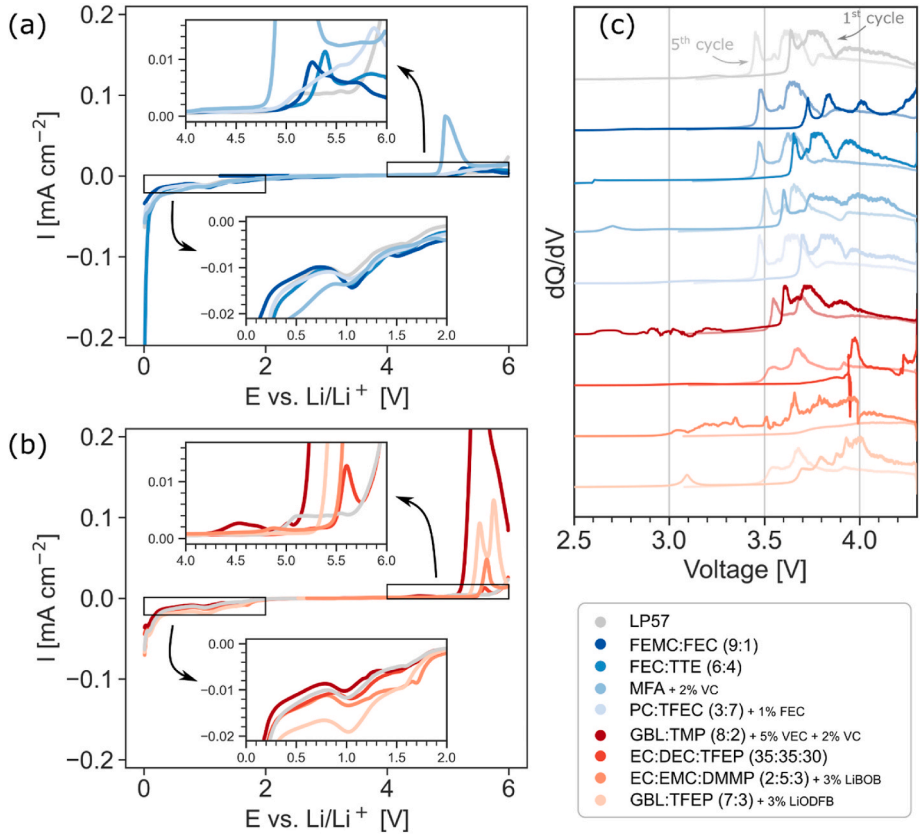

Fig. 1. Linear sweep voltammetry (LSV) of the (a) hydrofluorocarbon-based and (b) phosphate/phosphonate-based non-flammable electrolytes studied in this work. Anodic and cathodic sweeps were done using carbon-coated copper and carbon-coated aluminum working electrodes, respectively. (c) dQ/dV plots of the 1st and 5th cycles (at C/10) of NMC622|graphite containing each electrolyte.

them (70–80%). Passivation or corrosion of the aluminum also likely plays a significant role: starting at ca. 3.9 V vs Li/Li$^+$, $LiPF_6$ passivates Al current collectors to form an AlF_3 surface layer [46].

While LSV is a valuable technique to gain first insights into the electrochemical stability, it provides a simplified picture of electrolyte reactivity, as it neglects the role the active materials can play in catalyzing degradation processes [47]. The lattice oxygen atoms of NMC in particular are known to participate in the oxidation of solvent molecules, lowering the effective electrochemical stability limit considerably [48]. For instance, even though EC-based electrolytes often show little oxidative current against inert electrodes [49,50], when electrodes containing active materials are used, EC is the component that limits the oxidative stability of traditional electrolytes [51].

For a more realistic look at the redox activity of the electrolytes, the differential capacity plots of charging in NMC|graphite cells are plotted in Fig. 1c. The first cycle (during which the bulk of SEI formation occurs) and fifth cycle (by which time SEI formation is likely complete) are shown. These plots also contain peaks related to the intercalation of Li$^+$ into graphite and out of NMC622, in addition to reduction/oxidation peaks of the electrolyte. It is also not possible to directly compare them to the LSV plots, as they are recorded against a full cell potential, rather than a Li/Li$^+$ reference electrode. The dQ/dV data show substantial differences in reactivity among the electrolytes: the phosphate/phosphonates show significant decomposition peaks at much lower

potentials than the hydrofluorocarbons and LP57, although this is likely also due in part to the co-solvents used. By the fifth cycle, when SEI formation is presumed to be complete and the remaining peaks are likely due to the reversible Li/Li^+ redox, the redox behavior is more uniform redox across the electrolytes. The Li/Li^+ redox does show substantial overpotentials in the phosphates/phosphonates, as evidenced by the upshifted redox peak positions in the 5th cycle relative to the standard LP57. Conspicuously, EC:EMC:DMMP effects a complete breakdown in the characteristic Li/Li^+ redox peaks, indicating considerable electrochemical instability.

Fig. 2 shows long term cycling data of each electrolyte at a rate of C/2 (corresponding to ca. 80 mA g^{-1}). It is immediately evident that the four phosphate/phosphonate-containing electrolytes – GBL:TMP, EC:EMC:DMMP, EC:DEC:TFEP and GBL:TFEP (red traces) – perform significantly more poorly. All suffer from severe capacity fading in the first 10–20 cycles, accompanied by low initial coulombic efficiencies (Figs. S1 and S2), which only approach 100% after 50–100 cycles, implying inefficient SEI formation accompanied by high levels of lithium consumption. TMP and DMMP are believed to co-intercalate into graphite, causing its exfoliation [52,53]. The co-solvents and additives used evidently mitigate this phenomenon an extent, since TMP and DMMP on their own permit no reversible capacities at all, but may not be sufficient to prevent it entirely. The fluorinated phosphate TFEP, in contrast, has previously been shown not to undergo co-intercalation, which has been attributed to the lower electron density on the P═O bond and resulting weaker coordination of Li^+ [54]. However, as its poor cycling stability shows, it clearly suffers from some other problem – possibly a highly resistive SEI, as also suggested by its poor rate capability (Fig. 3). Interestingly, stable cycling with TFEP-based electrolytes in graphite-containing full cells has been reported when lithium nickel oxide or lithium nickel manganese oxide is used as the cathode [55,56], suggesting that the poor cycling stability described herein may be related to a specific incompatibility with NMC.

The phosphorus-free solvents (blue traces in Fig. 2), on the other hand, cycle much better, despite the fact that the non-flammable component or components of all four of these electrolytes are contained in much higher proportions than the phosphates. The organophosphorus moiety likely forms SEI components detrimental to performance (e.g., with low ionic conductivity or high electrical conductivity). The phosphorus-free compounds structurally resemble the proven carbonate-based electrolytes in wide use today and are more likely to produce effective SEIs.

Some of the co-solvents may also be partially responsible for the capacity decay; for instance, GBL and PC have known interfacial issues with graphite electrodes: GBL forms highly resistive SEIs on graphite [57] accompanied by high irreversible capacities [58], while PC forms no protective SEI at all but rather decomposes continuously, exfoliating the graphite structure [59]. TFEC may perform better when mixed with a different co-solvent. On the other hand, in the case of GBL:TMP it is plausible that the resistive SEI formed by GBL – if due to a thick or very dense structure – may be precisely what prevents the co-intercalation of TMP.

The poor cycling stability of the phosphate solvents is also reflected in their rate capability (Fig. 3): all exhibit noticeable capacity attrition even within the five cycles of each rate step, and have on average lower rate capabilities overall. The capacity decay caused by DMMP is so rapid, even at the lowest C-rate, that it drowns out the capacity loss caused by increasing the current density.

The internal resistance of each cell during battery cycling (Fig. 4) reinforces the cycling and rate capability results: the cells containing phosphates or phosphonates develop a higher resistance over time than those with hydrofluorocarbons. Even within each group, the resistance values are largely consistent with the rate capabilities. It is likely that SEI growth accounts for most of the increase in resistance, since all systems are identical except for the electrolyte, and probably explains at least in part the phosphate/phosphonate group's significantly poorer cycling stability.

It should be noted that the rate capability and ICI tests do not reflect fully identical conditions, as ICI is performed at much lower current densities. Some of the differences in rate capability are likely also related to the different reactivities of the electrolytes at high and low currents. For instance, cycling at high currents likely consumes less Li^+ in some electrolytes than others, or leads to the deposition of SEIs with different compositions and resistivities. The wide disparities in the C/10 capacities at the end of the rate tests (Fig. 3) suggests that a significant degree of SEI or electrolyte decomposition is taking place in some of the systems – and, again, more so among the phosphates/phosphonates than the hydrofluorocarbons.

The poor performance of phosphorus-containing solvents, which holds across a variety of metrics and co-solvents, is striking and suggests that this class of compounds suffers from fundamental electrochemical issues. For instance, organophosphate-derived SEI components may be intrinsically highly resistive, blocking the Li^+-conducting channels on the graphite surface. The uniformly higher internal resistances of the phosphate/phosphonate-containing cells suggest this as well. Traditional carbonate ester-based electrolytes are believed to form semicarbonates (alkyl carbonates) as the major ion-conducting species in SEIs; other salts like Li_2CO_3 can also contribute to ion conduction and

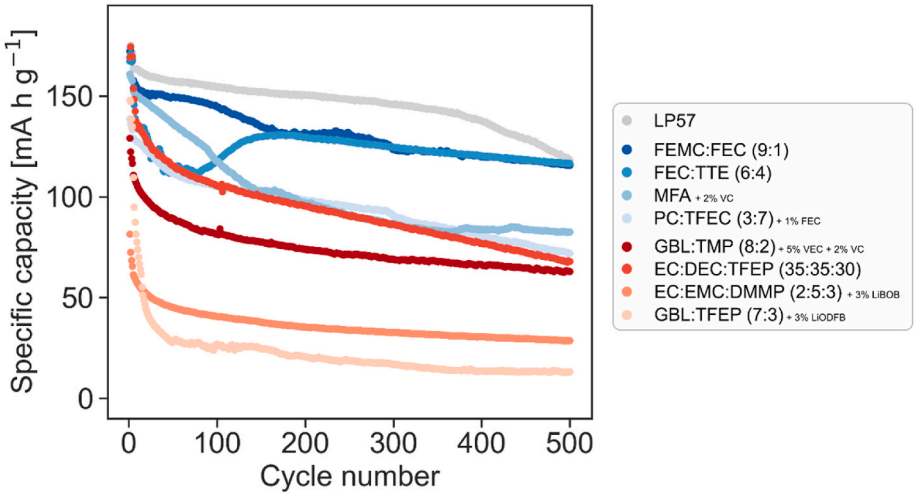

Fig. 2. Galvanostatic cycling performance of the non-flammable electrolytes studied in this work, grouped into phosphate/phosphonate-based and fluorinated carbonate/ester/ether-based, with LP57 shown as a benchmark.

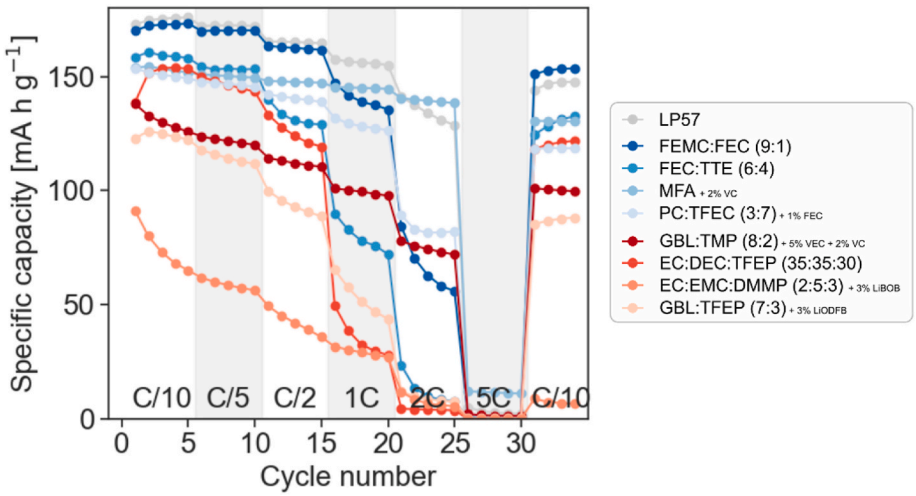

Fig. 3. Rate capability of the electrolytes based on organophosphorus compounds (red traces) and fluorinated carbonates, esters and ethers (blue traces). (For interpretation of the references to colour in this figure legend, the reader is referred to the Web version of this article.)

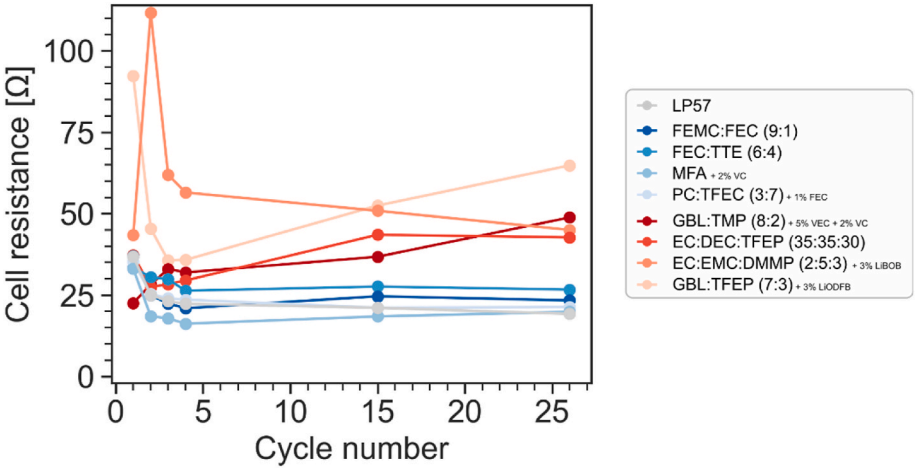

Fig. 4. Internal resistance of NMC622|graphite cells containing carious non-flammable electrolytes during cycling, as obtained by intermittent current interruption. Resistance values represent means during charge steps. Cycles 1–2, 15 and 26 (containing ICI steps) were carried out at a C-rate of C/10, while cycles 3–4 were carried out at C/5. Cycles 5–14 and 16–25 (without ICI) were carried out at a C-rate of C/2.

diffusion [60]. Phosphates and phosphonates, which lack a carbonyl moiety, cannot easily form these compounds; their major decomposition products during battery cycling are not known. If the O═PO_2R or O═PO_3 units of the phosphonates and phosphates end up forming significant parts of the SEI, it is unclear what their properties – e.g., ionic conductivity, solubility and mechanical strength – might be. On the other hand, the hydrofluorocarbons used in this work all contain ester or carbonate moieties and are more likely to form semicarbonate-like structures that enable Li^+-conduction.

3. Conclusions

In this work, eight promising non-flammable electrolytes – four based on phosphates or phosphonates and four based on hydrofluorocarbons – were selected from the existing literature, based on the criteria of previously demonstrated non-flammability, practical viability and wide use in the literature. All eight electrolytes were tested under identical conditions. Overall, the hydrofluorocarbons significantly outperformed the phosphates/phosphonates, exhibiting on average twice the capacity retention after 500 cycles, triple the rate capability as measured by the capacity at the fast charge-discharge rate of 2C, and half the cell resistance after 25 cycles. It is not straightforward to isolate the contribution of each electrolyte's non-flammable component to its overall electrochemical performance, since they contain a diverse range of co-solvents and additives. However, because these co-solvents and additives were selected to produce the most promising formulation (based on the existing literature) for each non-flammable solvent, it is possible to draw some broad conclusions. The most noticeable is the striking superiority of phosphorus-free fluorinated solvents over the phosphorus-containing ones, a trend that holds for all co-solvents used: even the "best" organophosphorus electrolyte, TFEP, underperforms the "worst" hydrofluorocarbon, TFEC. The intercalation into and exfoliation of graphite by TMP and DMMP presents a fundamental problem for which no practically viable solution has been found to date; the additives tested in this work are not sufficient. Given the environmental and economic concerns around fluorinated molecules, it would be worth trying to find a way to make these electrolytes viable. However, even TFEP, a phosphate which does not undergo co-intercalation, displayed significant capacity fading and growth in cell resistance, a trend observed with conventional (EC:DEC) as well as more experimental (GBL) co-solvents. This suggests that the use of phosphates may present general interfacial issues.

Finally, this study allows us to identify promising candidates for further study, as well as highlighting issues for in-depth investigation.

One obvious line of research would be to characterize the surfaces of the cycled electrodes and of the gas evolution during cycling, to gain an impression of the compounds making up the SEIs, and of the electrolyte decomposition reactions leading to them. There is also much scope for optimizing the performance of MFA and TFEC by experimenting with co-solvents and additives.

4. Experimental section

4.1. Electrolyte preparation

$LiPF_6$ and LP57 were purchased from Sigma Aldrich. Electrolyte solvent components were purchased from Tokyo Chemical Industry. All chemicals were used without further purification, aside from drying. Sample preparation was carried out in an MBraun glove box with O_2 content of less than 1.0 ppm and H_2O content of less than 1.5 ppm. Electrolytes were prepared by mixing all solvent components and drying over molecular sieves for at least 3 days, after which the liquid was filtered and 1 mol l^{-1} $LiPF_6$ added. $LiPF_6$ was dried at 70 °C under vacuum for 48 h before use.

4.2. Electrode preparation

Pre-fabricated electrode sheets of NMC622 ($LiNi_{0.6}Mn_{0.2}Co_{0.2}O_2$) coated on aluminium foil (foil thickness 20 μm) and artificial graphite coated onto copper foil (foil thickness 14 μm) were purchased from Custom Cells. Cathodes and anodes had areal capacities of 2.0 mA h cm^{-2} and 2.4 mA h g^{-1}, respectively; densities of 2.6 g cm^{-3} and 1.7 g cm^{-3}, respectively; and active material contents of 93.5% and 95%, respectively. Both electrodes also contained carbon black as conducting additives and PVDF binders (for the graphite) and CMC/SBR (for the NMC622). Circular electrodes with diameters of 13 mm were cut out and dried at 120 °C under vacuum for 12 h before use. Each cathode disk contained 16.8 mg of active material for a nominal capacity of 2.65 mA h. Each anode disk contained 19.9 mg of active material for a nominal capacity of 3.18 mA h. Electrode capacities were thus balanced for an anode:cathode ratio (N/P ratio) of 1.2.

4.3. Electrochemical measurements

Cycling and rate capability tests were performed at room temperature on a Neware cycler using 2-electrode NMC622|graphite pouch cells consisting of polymer-laminated aluminium. 24 mm × 24 mm squares of Celgard® 2400 (25 μm thick) were used as the separators, except for the trimethyl phosphate-containing electrolyte, for which glass fiber (ca. 100 μm thick) was used. 35 μl of solvent were applied to each side of the separator. All cells were rested for 5 h after assembly to allow the separators and electrodes to be fully wetted. CCCV cycling was used for cycling, rate capability and ICI experiments: each cell was charged at constant current (CC) to 4.3 V, after which the voltage was held at 4.3 V until the current reached 1/10 that of the current used during the preceding CC step. The cell was then discharged at constant current to 3 V. For long-term cycling, each cell was subjected to 2 cycles at C/10 (0.265 mA) and a further two at C/5 (0.53 mA) to allow SEI formation. Subsequent cycles were carried out at C/2 (1.325 mA). For rate capability experiments, no further formation cycles beyond the first five cycles at C/10 were carried out.

Intermittent current interruption experiments (ICI) were performed at room temperature on a Bio-Logic VMP3 potentiostat using 2-electrode NMC622|graphite CR2025 coin cells, using the method previously reported by Lacey et al. [61,62] Briefly, the procedure involves pausing a battery cell for very short periods of time at regular intervals; from the voltage response, the cell resistance can be calculated. In this work, 1 s pauses at 5-min intervals were used (except during the CV steps, which contained no interruptions). The resistance at each pause was calculated via

$$R = -\frac{\Delta V_{1s}}{I}$$

where I is the current before each interruption and ΔV_{1s} is the voltage drop 1 s after interruption. Because ICI experiments are most accurate under conditions close to equilibrium, they were carried out at C/10 or C/5 and interspersed with several non-ICI cycles at C/2 to simulate cell aging. To allow SEI formation, each cell was first subjected to 2 cycles at C/10 and two at C/5 under ICI conditions. Thereafter, each cell was cycled 10 times at C/2 without pausing, followed by 1 cycle at C/10 under ICI conditions, followed by another 10 cycles without pausing, and a final cycle at C/10 under ICI conditions. The sampling rate was 10 s^{-1} during interruptions and 1 min^{-1} during current application. The data were evaluated using an in-house Python script.

Linear sweep voltammetry (LSV) was carried out using 3-electrode pouch cells. Lithium metal disks (13 mm in diameter) were used as counter electrodes. Carbon-coated aluminum disks and carbon-coated copper disks (both 13 mm in diameter) were used as working electrodes for the cathodic and anodic sweeps, respectively. 27 mm × 27 mm squares of Celgard® 2400 were used as separators. Strips of lithium metal ca. 4 mm wide, placed close to but not between the active electrodes, were used as reference electrodes. To ensure the reference electrode did not come into contact with the working or counter electrodes, they were sandwiched between Celgard sheets. The sweep rate was 0.1 mV s^{-1}.

CRediT authorship contribution statement

Florian Gebert: Methodology, Investigation, Writing – original draft, Writing – review & editing, Visualization. **Matilde Longhini:** Investigation, Writing – review & editing. **Fosca Conti:** Resources, Writing – review & editing, Supervision. **Andrew J. Naylor:** Conceptualization, Methodology, Resources, Writing – review & editing, Supervision, Project administration, Funding acquisition.

Declaration of competing interest

The authors declare that they have no known competing financial interests or personal relationships that could have appeared to influence the work reported in this paper.

Data availability

Data will be made available on request.

Acknowledgements

The authors acknowledge financial support from the Swedish Energy Agency (project 51989-1) and STandUP for Energy for support to the Ångström Advanced Battery Centre.

Appendix A. Supplementary data

Supplementary data to this article can be found online at https://doi.org/10.1016/j.jpowsour.2022.232412.

References

[1] G. Sitty, N. Taft, What Will the Global Light-Duty Vehicle Fleet Look like through 2050? Fuel Freedom Foundation, 2016.
[2] H. Hao, X. Cheng, Z. Liu, F. Zhao, China's traction battery technology roadmap: targets, impacts and concerns, Energy Pol. 108 (2017) 355–358, https://doi.org/10.1016/j.enpol.2017.06.011.
[3] P. Sun, R. Bisschop, H. Niu, X. Huang, A review of battery fires in electric vehicles, Fire Technol. 56 (4) (2020) 1361–1410, https://doi.org/10.1007/s10694-019-00944-3.

[4] D.H. Doughty, Vehicle Battery Safety Roadmap Guidance, NREL/SR-5400-54404, 1055366, National Renewable Energy Laboratory, 2012, https://doi.org/10.2172/1055366.

[5] Y. Shigematsu, S. Kinoshita, M. Ue, Thermal behavior of a C / LiCoO2 cell, its components, and their combinations and the effects of electrolyte additives, J. Electrochem. Soc. 153 (11) (2006), A2166, https://doi.org/10.1149/1.2347100.

[6] T. Inoue, K. Mukai, Roles of positive or negative electrodes in the thermal runaway of lithium-ion batteries: accelerating rate calorimetry analyses with an all-inclusive microcell, Electrochem. Commun. 77 (2017) 28–31, https://doi.org/10.1016/j.elecom.2017.02.008.

[7] L. Kong, C. Li, J. Jiang, M.G. Pecht, Li-ion battery fire hazards and safety strategies, Energies 11 (9) (2018) 2191, https://doi.org/10.3390/en11092191.

[8] R. Bisschop, O. Willstrand, F. Amon, M. Rosengren, RI.SE Report, Fire Safety of LithiumIon Batteries in Road Vehicles, vol. 106, 2019.

[9] R. Gond, W. van Ekeren, R. Mogensen, J. Naylor, R.A. Younesi, Non-flammable liquid electrolytes for safe batteries, Mater. Horiz. 8 (11) (2021) 2913–2928, https://doi.org/10.1039/D1MH00748C.

[10] G.G. Eshetu, J.-P. Bertrand, A. Lecocq, S. Grugeon, S. Laruelle, M. Armand, G. Marlair, Fire behavior of carbonates-based electrolytes used in Li-ion rechargeable batteries with a focus on the role of the LiPF6 and LiFSI salts, J. Power Sources 269 (2014) 804–811, https://doi.org/10.1016/j.jpowsour.2014.07.065.

[11] I. Dincer, M.A. Rosen, F. Khalid, Thermal energy production, in: I. Dincer (Ed.), Comprehensive Energy Systems, Elsevier, Oxford, 2018, pp. 673–706, https://doi.org/10.1016/B978-0-12-809597-3.00335-7.

[12] A. Mauger, C.M. Julien, A. Paolella, M. Armand, K. Zaghib, Building better batteries in the solid state: a review, Materials 12 (23) (2019) 3892, https://doi.org/10.3390/ma12233892.

[13] E. Jónsson, Ionic liquids as electrolytes for energy storage applications – a modelling perspective, Energy Storage Mater. 25 (2020) 827–835, https://doi.org/10.1016/j.ensm.2019.08.030.

[14] X. Liu, X. Shen, F. Zhong, X. Feng, W. Chen, X. Ai, H. Yang, Y. Cao, Enabling electrochemical compatibility of non-flammable phosphate electrolytes for lithium-ion batteries by tuning their molar ratios of salt to solvent, Chem. Commun. 56 (48) (2020) 6559–6562, https://doi.org/10.1039/D0CC02940H.

[15] R. Mogensen, S. Colbin, A.S. Menon, E. Björklund, R. Younesi, Sodium bis(Oxalato) Borate in trimethyl phosphate: a fire-extinguishing, fluorine-free, and low-cost electrolyte for full-cell sodium-ion batteries, ACS Appl. Energy Mater. 3 (5) (2020) 4974–4982, https://doi.org/10.1021/acsaem.0c00522.

[16] L.O.S. Colbin, R. Mogensen, A. Buckel, Y.-L. Wang, A.J. Naylor, J. Kullgren, R. Younesi, A halogen-free and flame-retardant sodium electrolyte compatible with hard carbon anodes, Adv. Mater. Interfac. 8 (23) (2021), 2101135, https://doi.org/10.1002/admi.202101135.

[17] S. Caron, Where does the fluorine come from? A review on the challenges associated with the synthesis of organofluorine compounds, Org. Process Res. Dev. 24 (4) (2020) 470–480, https://doi.org/10.1021/acs.oprd.0c00030.

[18] M. Zackrisson, S. Schellenberger, Toxicity of Lithium Ion Battery Chemicals - Overview with Focus on Recycling, RISE IVF Project Report, 2020.

[19] Y. Yamada, J. Wang, S. Ko, E. Watanabe, A. Yamada, Advances and issues in developing salt-concentrated battery electrolytes, Nat. Energy 4 (4) (2019) 269–280, https://doi.org/10.1038/s41560-019-0336-z.

[20] S. Hess, M. Wohlfahrt-Mehrens, M. Wachtler, Flammability of Li-ion battery electrolytes: flash point and self-extinguishing time measurements, J. Electrochem. Soc. 162 (2) (2015), A3084, https://doi.org/10.1149/2.0121502jes.

[21] J. Im, J. Lee, M.-H. Ryou, Y.M. Lee, K.Y. Cho, Fluorinated carbonate-based electrolyte for high-voltage Li(Ni0.5Mn0.3Co0.2)O2/graphite lithium-ion battery, J. Electrochem. Soc. 164 (1) (2017), A6381, https://doi.org/10.1149/2.0591701jes.

[22] J. Hou, L. Wang, X. Feng, J. Terada, L. Lu, S. Yamazaki, A. Su, Y. Kuwajima, Y. Chen, T. Hidaka, X. He, H. Wang, O. Minggao, Thermal runaway of lithium-ion batteries employing flame-retardant fluorinated electrolytes, Energy Environ. Mater. (2021), https://doi.org/10.1002/eem2.12297.

[23] X. Fan, L. Chen, O. Borodin, X. Ji, J. Chen, S. Hou, T. Deng, J. Zheng, C. Yang, S.-C. Liou, K. Amine, K. Xu, C. Wang, Non-flammable electrolyte enables Li-metal batteries with aggressive cathode chemistries, Nat. Nanotechnol. 13 (8) (2018) 715–722, https://doi.org/10.1038/s41565-018-0183-2.

[24] C. Wu, Y. Wu, X. Yang, T. Xin, S. Chen, M. Yang, Y. Peng, H. Xu, Y. Yin, T. Deng, X. Feng, Thermal runaway suppression of high-energy lithium-ion batteries by designing the stable interphase, J. Electrochem. Soc. 168 (9) (2021), 090563, https://doi.org/10.1149/1945-7111/ac285f.

[25] J.-I. Yamaki, I. Yamazaki, M. Egashira, S. Okada, Thermal studies of fluorinated ester as a novel candidate for electrolyte solvent of lithium metal anode rechargeable cells, J. Power Sources 102 (1) (2001) 288–293, https://doi.org/10.1016/S0378-7753(01)00805-9.

[26] M. Ihara, B.T. Hang, K. Sato, M. Egashira, S. Okada, J. Yamaki, Properties of carbon anodes and thermal stability in LiPF6/methyl difluoroacetate electrolyte, J. Electrochem. Soc. 150 (11) (2003), A1476, https://doi.org/10.1149/1.1614269.

[27] T. Kawamura, T. Tanaka, M. Egashira, I. Watanabe, S. Okada, J. Yamaki, Methyl difluoroacetate inhibits corrosion of aluminum cathode current collector for lithium ion cells, Electrochem. Solid State Lett. 8 (9) (2005) A459, https://doi.org/10.1149/1.1993367.

[28] L. Zhao, S. Okada, J. Yamaki, Effect of VC additive on MFA-based electrolyte in Li-ion batteries, J. Power Sources 244 (2013) 369–374, https://doi.org/10.1016/j.jpowsour.2012.12.098.

[29] K. Sato, L. Zhao, S. Okada, J. Yamaki, LiPF6/Methyl difluoroacetate electrolyte with vinylene carbonate additive for Li-ion batteries, J. Power Sources 196 (13) (2011) 5617–5622, https://doi.org/10.1016/j.jpowsour.2011.02.068.

[30] T. Tanaka, T. Doi, S. Okada, J. -i. Yamaki, Effects of salts in methyl difluoroacetate-based electrolytes on their thermal stability in lithium-ion batteries, Fuel Cell. 9 (3) (2009) 269–272, https://doi.org/10.1002/fuce.200800085.

[31] T. Doi, R. Matsumoto, T. Endo, Z. Cao, T. Sato, M. Haruta, M. Hashinokuchi, Y. Kimura, M. Inaba, Extension of anodic potential window of ester-based electrolyte solutions for high-voltage lithium ion batteries, ACS Appl. Energy Mater. 2 (11) (2019) 7728–7732, https://doi.org/10.1021/acsaem.9b01334.

[32] H.Q. Pham, E.-H. Hwang, Y.-G. Kwon, S.-W. Song, Approaching the maximum capacity of nickel-rich LiNi0.8Co0.1Mn0.1O2 cathodes by charging to high-voltage in a non-flammable electrolyte of propylene carbonate and fluorinated linear carbonates, Chem. Commun. 55 (9) (2019) 1256–1258, https://doi.org/10.1039/C8CC10017A.

[33] H.Q. Pham, H.-Y. Lee, E.-H. Hwang, Y.-G. Kwon, S.-W. Song, Non-flammable organic liquid electrolyte for high-safety and high-energy density Li-ion batteries, J. Power Sources 404 (2018) 13–19, https://doi.org/10.1016/j.jpowsour.2018.09.075.

[34] P. Murmann, X. Mönnighoff, N. von Aspern, P. Janssen, N. Kalinovich, M. Shevchuk, O. Kazakova, G.-V. Röschenthaler, I. Cekic-Laskovic, M. Winter, Influence of the fluorination degree of organophosphates on flammability and electrochemical performance in lithium ion batteries: studies on fluorinated compounds deriving from triethyl phosphate, J. Electrochem. Soc. 163 (5) (2016) A751, https://doi.org/10.1149/2.1031605jes.

[35] K. Xu, S. Zhang, J.L. Allen, T.R. Jow, Nonflammable electrolytes for Li-ion batteries based on a fluorinated phosphate, J. Electrochem. Soc. 149 (8) (2002) A1079, https://doi.org/10.1149/1.1490356.

[36] Y.M. Todorov, M. Aoki, H. Mimura, K. Fujii, N. Yoshimoto, M. Morita, Thermal and electrochemical properties of nonflammable electrolyte solutions containing fluorinated alkylphosphates for lithium-ion batteries, J. Power Sources 332 (2016) 322–329, https://doi.org/10.1016/j.jpowsour.2016.09.119.

[37] M.S. Ding, K. Xu, T.R. Jow, Effects of tris(2,2,2-trifluoroethyl) phosphate as a flame-retarding cosolvent on physicochemical properties of electrolytes of LiPF6 in EC-PC-EMC of 3:3:4 weight ratios, J. Electrochem. Soc. 149 (11) (2002), A1489, https://doi.org/10.1149/1.1513556.

[38] Y. Gu, S. Fang, L. Yang, S. Hirano, Tris(2,2,2-Trifluoroethyl) phosphate as a cosolvent for a nonflammable electrolyte in lithium-ion batteries, ACS Appl. Energy Mater. 4 (5) (2021) 4919–4927, https://doi.org/10.1021/acsaem.1c00503.

[39] Y. Shigematsu, M. Ue, J. Yamaki, Thermal behavior of charged graphite and Li x CoO2 in electrolytes containing alkyl phosphate for lithium-ion cells, J. Electrochem. Soc. 156 (3) (2009) A176, https://doi.org/10.1149/1.3056035.

[40] X. Wang, E. Yasukawa, S. Kasuya, Nonflammable trimethyl phosphate solvent-containing electrolytes for lithium-ion batteries: I. Fundamental properties, J. Electrochem. Soc. 148 (10) (2001) A1058, https://doi.org/10.1149/1.1397773.

[41] X.L. Yao, S. Xie, C.H. Chen, Q.S. Wang, J.H. Sun, Y.L. Li, S.X. Lu, Comparative study of trimethyl phosphite and trimethyl phosphate as electrolyte additives in lithium ion batteries, J. Power Sources 144 (1) (2005) 170–175, https://doi.org/10.1016/j.jpowsour.2004.11.042.

[42] K. Xu, M.S. Ding, S. Zhang, J.L. Allen, T.R. Jow, An attempt to formulate nonflammable lithium ion electrolytes with alkyl phosphates and phosphazenes, J. Electrochem. Soc. 149 (5) (2002) A622, https://doi.org/10.1149/1.1467946.

[43] H. Ota, A. Kominato, W.-J. Chun, E. Yasukawa, S. Kasuya, Effect of cyclic phosphate additive in non-flammable electrolyte, J. Power Sources 119–121 (2003) 393–398, https://doi.org/10.1016/S0378-7753(03)00259-3.

[44] S. Dalavi, M. Xu, B. Ravdel, L. Zhou, B.L. Lucht, Nonflammable electrolytes for lithium-ion batteries containing dimethyl methylphosphonate, J. Electrochem. Soc. 157 (10) (2010), A1113, https://doi.org/10.1149/1.3473828.

[45] H.F. Xiang, H.Y. Xu, Z.Z. Wang, C.H. Chen, Dimethyl methylphosphonate (DMMP) as an efficient flame retardant additive for the lithium-ion battery electrolytes, J. Power Sources 173 (1) (2007) 562–564, https://doi.org/10.1016/j.jpowsour.2007.05.001.

[46] T. Ma, G.-L. Xu, Y. Li, L. Wang, X. He, J. Zheng, J. Liu, M.H. Engelhard, P. Zapol, L. A. Curtiss, J. Jorne, K. Amine, Z. Chen, Revisiting the corrosion of the aluminum current collector in lithium-ion batteries, J. Phys. Chem. Lett. 8 (5) (2017) 1072–1077, https://doi.org/10.1021/acs.jpclett.6b02933.

[47] K. Xu, S.P. Ding, T.R. Jow, Toward reliable values of electrochemical stability limits for electrolytes, J. Electrochem. Soc. 146 (11) (1999) 4172, https://doi.org/10.1149/1.1392609.

[48] R. Jung, M. Metzger, F. Maglia, C. Stinner, H.A. Gasteiger, Chemical versus electrochemical electrolyte oxidation on NMC111, NMC622, NMC811, LNMO, and conductive carbon, J. Phys. Chem. Lett. 8 (19) (2017) 4820–4825, https://doi.org/10.1021/acs.jpclett.7b01927.

[49] Z. Khodr, C. Mallet, J.-C. Daigle, Z. Feng, K. Amouzegar, J. Claverie, K. Zaghib, Electrochemical study of functional additives for Li-ion batteries, J. Electrochem. Soc. 167 (12) (2020), 120535, https://doi.org/10.1149/1945-7111/abae92.

[50] B. Aktekin, G. Hernández, R. Younesi, D. Brandell, K. Edström, Concentrated LiFSI–ethylene carbonate electrolytes and their compatibility with high-capacity and high-voltage electrodes, ACS Appl. Energy Mater. 5 (1) (2022) 585–595, https://doi.org/10.1021/acsaem.1c03096.

[51] J. Xia, R. Petibon, D. Xiong, L. Ma, J.R. Dahn, Enabling linear alkyl carbonate electrolytes for high voltage Li-ion cells, J. Power Sources 328 (2016) 124–135, https://doi.org/10.1016/j.jpowsour.2016.08.015.

[52] H. Nakagawa, M. Ochida, Y. Domi, T. Doi, S. Tsubouchi, T. Yamanaka, T. Abe, Z. Ogumi, Electrochemical Raman study of edge plane graphite negative-electrodes

in electrolytes containing trialkyl phosphoric ester, J. Power Sources 212 (2012) 148–153, https://doi.org/10.1016/j.jpowsour.2012.04.013.
[53] J.K. Feng, X.J. Sun, X.P. Ai, Y.L. Cao, H.X. Yang, Dimethyl methyl phosphate: a new nonflammable electrolyte solvent for lithium-ion batteries, J. Power Sources 184 (2) (2008) 570–573, https://doi.org/10.1016/j.jpowsour.2008.02.006.
[54] H. Nakagawa, Y. Domi, T. Doi, M. Ochida, S. Tsubouchi, T. Yamanaka, T. Abe, Z. Ogumi, In situ Raman study of graphite negative-electrodes in electrolyte solution containing fluorinated phosphoric esters, J. Electrochem. Soc. 161 (4) (2014) A480, https://doi.org/10.1149/2.007404jes.
[55] K. Xu, S. Zhang, J.L. Allen, T.R. Jow, Evaluation of fluorinated alkyl phosphates as flame retardants in electrolytes for Li-ion batteries: II. Performance in cell, J. Electrochem. Soc. 150 (2) (2003) A170, https://doi.org/10.1149/1.1533041.
[56] Z. Zeng, X. Liu, X. Jiang, Z. Liu, Z. Peng, X. Feng, W. Chen, D. Xia, X. Ai, H. Yang, Y. Cao, Enabling an intrinsically safe and high-energy-density 4.5 V-class Li-ion battery with nonflammable electrolyte, InfoMat 2 (5) (2020) 984–992, https://doi.org/10.1002/inf2.12089.
[57] J. Ufheil, M.C. Baertsch, A. Würsig, P. Novák, Maleic anhydride as an additive to γ-butyrolactone solutions for Li-ion batteries, Electrochim. Acta 50 (7) (2005) 1733–1738, https://doi.org/10.1016/j.electacta.2004.10.061.
[58] K. Xu, Tailoring electrolyte composition for LiBOB, J. Electrochem. Soc. 155 (10) (2008) A733, https://doi.org/10.1149/1.2961055.
[59] L. Xing, X. Zheng, M. Schroeder, J. Alvarado, A. von Wald Cresce, K. Xu, Q. Li, W. Li, Deciphering the ethylene carbonate–propylene carbonate mystery in Li-ion batteries, Acc. Chem. Res. 51 (2) (2018) 282–289, https://doi.org/10.1021/acs.accounts.7b00474.
[60] S. Shi, Y. Qi, H. Li, L.G. Hector, Defect thermodynamics and diffusion mechanisms in Li2CO3 and implications for the solid electrolyte interphase in Li-ion batteries, J. Phys. Chem. C 117 (17) (2013) 8579–8593, https://doi.org/10.1021/jp310591u.
[61] M.J. Lacey, Influence of the electrolyte on the internal resistance of Lithium−Sulfur batteries studied with an intermittent current interruption method, Chemelectrochem 4 (8) (2017) 1997–2004, https://doi.org/10.1002/celc.201700129.
[62] Z. Geng, T. Thiringer, M.J. Lacey, Intermittent current interruption method for commercial lithium-ion batteries aging characterization, IEEE Trans. Transport. Electrification 8 (2) (2022) 2985–2995, https://doi.org/10.1109/TTE.2021.3125418.

Glossary

ARC: accelerated rate calorimetry
DEC: diethyl carbonate
DMC: dimethyl carbonate
DMMP: dimethyl methylphosphonate
DSC: differential scanning calorimetry
EC: ethylene carbonate
EMC: ethyl methylcarbonate
EV: electric vehicle
FEC: fluoroethylene carbonate
FEMC: 2,2,2-trifluoroethyl methyl carbonate
FP: flash point
GBL:: γ-butyrolactone
ICI: intermittent current interruption
LIB: lithium-ion battery
LiBOB: lithium bis(oxalato)borate
LiODFB: lithium difluoro(oxalate) borate
LSV: linear sweep voltammetry
MFA: methyl difluoroacetate
NMC622: $LiNi_{0.6}Mn_{0.2}Co_{0.2}O_2$
PC: propylene carbonate
SEI: solid-electrolyte interphase
SET: self-extinguishing time
TFEC: bis(2,2,2-trifluoroethyl) carbonate
TFEP: tris(2,2,2-trifluoroethyl) phosphate
TMP: trimethyl phosphate
TTE: 1,1,2,2-tetrafluoroethyl-2,2,3,3-tetrafluoropropylether
VC: vinylene carbonate
VEC: vinyl ethylene carbonate